Collective-Goldstone-mode-induced ultralow lattice thermal conductivity in Sn-filled skutterudite SnFe_{4}Sb_{12}

Yuhao Fu, Xin He, Lijun Zhang, and David J. Singh

Collective Goldstone mode induced ultralow lattice thermal conductivity in Sn-filled skutterudite SnFe$_4$Sb$_{12}$

Yuhao Fu[1,2], Xin He[1], Lijun Zhang[1],* and David J. Singh[2†]

[1]*State Key Laboratory of Superhard Materials, Key Laboratory of Automobile Materials of MOE,*
and College of Materials Science and Engineering, Jilin University, Changchun 130012, China and
[2]*Department of Physics and Astronomy, University of Missouri, Columbia, MO 65211-7010, USA*

We demonstrate that the concept of Goldstone bosons can be exploited for phonon control and thermal conductivity reduction of materials. By studying lattice dynamics of the Sn filled skutterudite SnFe$_4$Sb$_{12}$, we find Sn off-centers in its coordination cage in contrast to the common rare earth fillers. This leads to low-frequency Goldstone-like modes below 1 THz associated mainly with Sn motions. Importantly, these involve collective motion of other atoms, especially Sb, in the host skutterudite lattice. The optical modes transverse to the Sn off-centering direction are identified as Goldstone type modes in association with a three-dimensional Mexican hat-like potential energy surface. The interaction of these collective Goldstone modes with the host heat-carrying phonons is shown to lead to ultralow thermal conductivities.

I. INTRODUCTION

Goldstone modes are bosons that appear in models with spontaneous breaking of continuous symmetries.[1,2] While originally discussed in the context of superconductivity and particle physics, they can also occur in lattice dynamics, and were observed by polarized Raman scattering in pyrochlore Cd$_2$Re$_2$O$_7$.[3] In this material the symmetry breaking is the breaking of cubic symmetry by simple off-centering of the Cd ions in their cages. Here we show that more complex collective Goldstone-like modes occur in the filled skutterudite SnFe$_4$Sb$_{12}$ and that these modes result in an exceptionally strong reduction of the thermal conductivity. In SnFe$_4$Sb$_{12}$ the Goldstone modes have mixed character involving the filling atom and the Sb atoms that coordinate it, distinct from Cd$_2$Re$_2$O$_7$, and important for the lowering of the thermal conductivity.

Filled skutterudites, exemplified by BaCo$_4$Sb$_{12}$ and LaFe$_4$Sb$_{12}$, have provided both a number of important thermoelectric compositions and a rich model system for understanding transport in materials.[4–10] The unfilled skutterudite, CoSb$_3$, has a relatively high thermal conductivity, which is strongly reduced by filling of the icosahedral voids in the structure with alkaline earth, rare earth and other elements. For filled skutterudites there is a complex and not yet fully understood interplay between the modified electronic properties by filling and effects of the fillers on thermal conductivity. These are both direct through introduction of new filler-derived vibrational modes and indirect through modifications of the electronic structure and thereby charges in the bonding of the host lattice. Properties of skutterudites are highly sensitive to electron count,[11–14] which in turn can be tuned by charge donation from the filling site, by metal site (Fe,Co) alloying and by control of the defect chemistry.[14–21]

Relevant to electron count, there are two classes of skutterudite filler atoms: highly electropositive fillers, such as alkaline, alkaline earth and rare earth elements, whose bonding, stability and electronic properties can be understood in terms of Zintl charge transfer to the host lattice,[21] and chemically active fillers such as Tl, In, and Sn.[22] Here we focus on the Sn filled compound SnFe$_4$Sb$_{12}$, which has been experimentally synthesized in thin film form.[23] The corresponding Co-based compound can be made in bulk form by high pressure synthesis, and has properties that indicate potential as a good thermoelectric material.[24] These are distinct from Sn substitution on the Sb site, which is also possible by controlling synthesis conditions.[16]

We find that the Sn in SnFe$_4$Sb$_{12}$ behaves differently from other fillers in that it strongly off-centers to form three-fold bonds with Sb having a covalent nature. This bonding arrangement gives rise to a novel lattice dynamics associated with Sn, which shows low-frequency optic branches that can be characterized as Goldstone-like modes. This is in the sense that these modes correspond to the Sn motion perpendicular to the off-centering direction in an effective potential energy surface with three-dimensional Mexican hat shape. We find that this lattice dynamics leads to an exceptionally low thermal conductivity, well below that of most other filled skutterudites.

II. APPROACH

Our results are based on density functional calculations.[25] The equilibrium crystal structures and electronic properties were obtained with the plane-wave projector-augmented-wave method[26], as implemented in the VASP code[27]. We used high-quality potentials in which the 3d and 4s (Fe), 5s and 5p (Sb), 4d, 5s and 5p (Sn), and 5s, 5p, 5d and 6s (La) electrons were treated explicitly as valence electrons. We used the local density approximation (LDA) for the exchange-correlation functional. This was done to avoid any artifacts due to the tendency of commonly used generalized gradient approximations functionals to slightly overestimate lattice parameters, which can
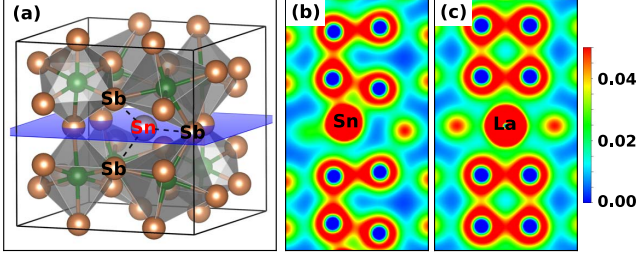
FIG. 1. (a) Structure of $SnFe_4Sb_{12}$ (space group Cm) obtained by total energy minimization. Sn off-centers and bonds with three Sb atoms. Sn is located in the (001) plane (blue) comprised of four Sb. (b, c) Charge density in the (001) plane showing the Sb_4 ring and the fillers in $SnFe_4Sb_{12}$ and $LaFe_4Sb_{12}$. The color range is from 0 (blue) to 0.05 (red) electron/$Å^3$.

lead to overly soft modes in some materials with heavy atoms, an example being the ferroelectric $PbTiO_3$.[28] This is important to current study because incorrect soft modes could artificially lower the thermal conductivity.

Structural optimizations were done with a kinetic energy cutoff of 350 eV and Brillouin zone integration via k-point meshes of spacing $2\pi \times 0.03$ $Å^{-1}$ or less. Harmonic phonons were calculated using the real-space supercell approach as implemented in the PHONOPY code[29]. The lattice thermal conductivity κ_l was calculated by iteratively solving the linearized Boltzmann-Peierls transport equation for phonons as implemented in the ShengBTE package[30–32]. Further details of the computational procedures are in the Supplementary Materials.[33]

III. STRUCTURE AND BONDING

The optimized structure of $SnFe_4Sb_{12}$ shows the Sn off-centered in its cage of Sb as shown in Fig. 1a. This is accompanied by the formation of three-fold Sn-Sb bonds with the bond lengths of 2.87 Å, 2.92 Å, and 2.92 Å. The charge density (Fig. 1b) shows both a degree of covalency between Sn and Sb as well as a change in the bonding of the Sb_4 rings characterizing the skutterudite structure (note the bonds among the Sb atoms with one bond noticably depleted). In contrast, for $LaFe_4Sb_{12}$ with the centered La filler (Fig. 1c) the interaction between La and Sb is practically completely ionic, resulting in undisturbed bonding of the Sb_4 rings.

IV. ENERGY SURFACE

In spite of the fact that the optimized structure of $SnFe_4Sb_{12}$ shows off-centered Sn, we do not find an off-centering for Sn if the other atoms in the skutterudite framework are held fixed at their undistorted positions. Calculation of the energy as a function of Sn
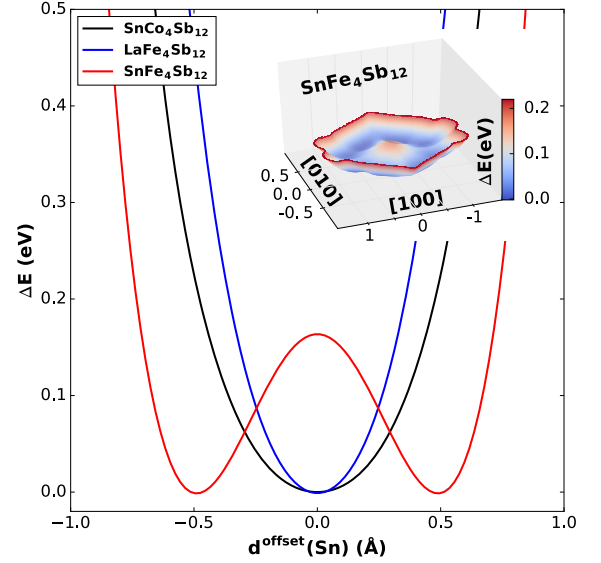

FIG. 2. Calculated effective potential wells for Sn off-centering with constrained relaxation (see text) for $SnCo_4Sb_{12}$, $LaFe_4Sb_{12}$ and $SnFe_4Sb_{12}$. The inset shows the effective potential surface in the indicated (001) plane (shown in blue in Fig. 1a) for $SnFe_4Sb_{12}$.

position, while keeping the other atoms in the unit cell fixed, show a stable Sn location at the center of the cage. The obtained structure is similar to the stable cubic filled skutterudites with the centred fillers, $LaFe_4Sb_{12}$ and $SnCo_4Sb_{12}$. The implication is that the off-centering of Sn and the distortion of cubic $SnFe_4Sb_{12}$ require collective motion of Sn and the neighboring atoms. Therefore Sn motion couples strongly to the host skutterudite lattice and induces distortion in it. This is as may be anticipated from Fig. 1b, where the charge density shows that interaction of Sb with its neighboring Sn affects bonding of this Sb with neighboring Sb in the Sb_4 ring. Within a rattling ion picture, the motion of Sn is then expected to be strongly coupled to (i.e. mixed with) the host lattice vibrations. This expectation is also consistent with Raman scattering results for the Co analogue, $SnCo_4Sb_{12}$.[34]

V. LATTICE DYNAMICS

To probe lattice dynamics of the Sn off-centering, we calculate the potential well for Sn motion in $SnFe_4Sb_{12}$. In particular we start with the symmetric filled skutterudite, fully relaxed with cubic symmetry (i.e. with filler in the center of the cage), off-center the filler and then relax again with the constraint that the shortest Sn-Sb bond length is kept fixed. The result is plotted in Fig. 2, comparing $LaFe_4Sb_{12}$ and $SnCo_4Sb_{12}$. As seen, while $LaFe_4Sb_{12}$ and $SnCo_4Sb_{12}$ show similar single-well profiles, there is a clear double-well potential for $SnFe_4Sb_{12}$. By scanning the Sn positions within the plane shown in

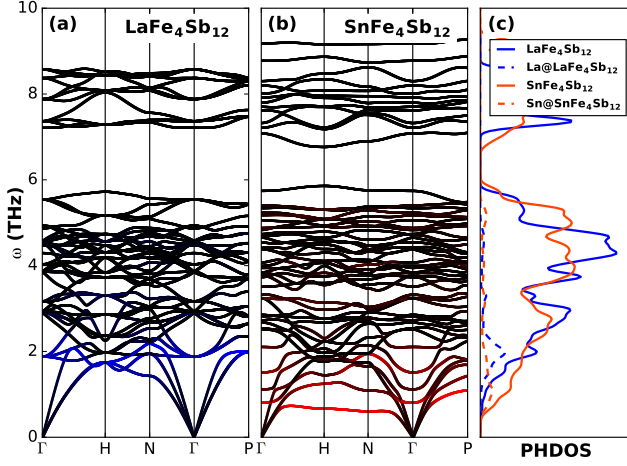FIG. 3. Calculated phonon dispersion of (a) LaFe$_4$Sb$_{12}$ and (b) SnFe$_4$Sb$_{12}$. For a clear comparison between two compounds, we chose phonon momentum vectors in the BCC Brillouin zone of skutterudites, even though the actual structure of SnFe$_4$Sb$_{12}$ is monoclinic (Fig. 1). Blue and red lines represent the projections onto La and Sn, respectively. (c) Calculated phonon density of states (PHDOS), with LaFe$_4$Sb$_{12}$ and SnFe$_4$Sb$_{12}$ shown in blue and red, respectively. The dashed lines represent the projections onto the filler atoms.
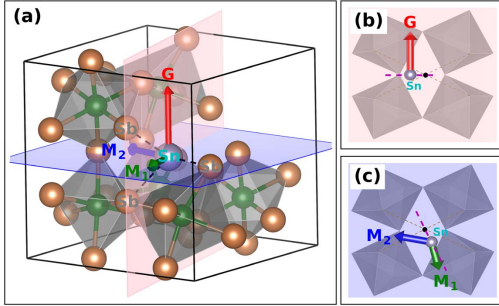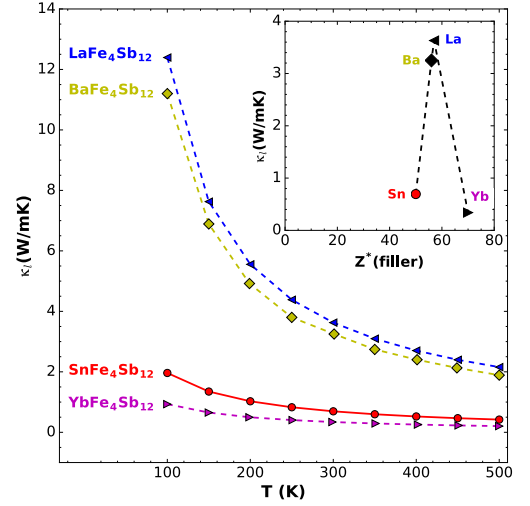

FIG. 5. Calculated temperature dependence of lattice thermal conductivity κ_l (in W/mK) of SnFe$_4$Sb$_{12}$, compared with other fully filled skutterudites (LaFe$_4$Sb$_{12}$, BaFe$_4$Sb$_{12}$[40], YbFe$_4$Sb$_{12}$[40]). The inset shows the κ_l value at 300 K vs the filler atomic number (Z*).

FIG. 4. (a) Calculated phonon eigenvectors of the first three optical branches at Γ for SnFe$_4$Sb$_{12}$, depicted by the red (first), green (second) and blue (third) arrows, respectively. The pink and blue planes represent the planes containing the first phonon eigenvector, the second and third phonon eigenvectors, respectively. (b) and (c) show the phonon eigenvectors within two planes in (a). The edge-sharing FeSb$_6$ octahedra are shown to represent the skutterudite framework. The purple line refers to the Sn off-centering direction. G represents a Goldstone mode, and M$_1$, M$_2$ mean the mixed-character (with both Higgs and Goldstone character, i.e. mixed radial and transverse components) modes.

Fig. 1, we get a three-dimensional potential energy surface with a Mexican hat-like shape (inset of Fig. 2). This suggests existence of collective Goldstone modes[1,2] associated with Sn motions transverse to the off-centering direction (by collective we mean that they involve both Sn and the cage atoms from skutterudite framework, distinct from modes seen in Cd$_2$Re$_2$O$_7$[3]).

Calculated phonon dispersions of the filler-centered LaFe$_4$Sb$_{12}$ and the filler-off-centered SnFe$_4$Sb$_{12}$ are shown in Fig. 3, along with the corresponding phonon densities of states. As seen in the density of states (Fig. 3c), Sn introduces vibrational modes over a wider frequency range, and extends down to much lower frequency than La. This comes from the first three optical phonon branches at low frequency (red curves in Fig. 3b), which are generally lower in frequency than the La-derived modes (blue curves in Fig. 3a). Also these Sn-derived optical modes fall below the maximum of the transverse acoustic branches (see $e.g.$ the Γ-H direction). The lowest mode has a frequency as low as 0.79 THz, which is even lower than the case of the quite heavy filler of Yb (1.11 THz) calculated in the same way.[14]

The phonon eigenvectors of the first three Sn-derived optical branches at Γ for SnFe$_4$Sb$_{12}$ are depicted in Fig. 4. In terms of specific vibration patterns, these modes can be assigned to the Goldstone type mode (transverse to the Sn off-centering direction) or the Higgs type mode (along the Sn off-centering direction).[1,2,35–37] The lowest mode (the G in Fig. 4b) has Goldstone character, with an eigenvector along the bottom of the Mexican hat-like energy surface. The other two (the M$_1$ and M$_2$ as in Fig. 4c) have mixed character as discussed in analogous physical systems.[37–39] Here it is due to the distortion of the potential energy surface shape from a perfectly flat bottom of the Mexican hat (inset of Fig. 2). Note that the symmetry breaking due to the Sn off-centering plays the essential role in the formation of these distinct modes. With cubic symmetry, one obtains a single three fold degenerate optic mode at Γ.

VI. THERMAL CONDUCTIVITY

The lattice thermal conductivities κ_l are shown in Fig. 5. As seen, $SnFe_4Sb_{12}$ has an ultralow thermal conductivity, much lower than $LaFe_4Sb_{12}$, which is the prototypical filled skutterudite thermoelectric, with low thermal conductivity due to the La filling, as well as $BaFe_4Sb_{12}$[40]. The values are comparable to those of $YbFe_4Sb_{12}$. This is a useful reference since it has the lowest thermal conductivity among the high performance single filled skutterudites. Our result strongly violates the generally accepted tendency that the heavier filler in skutterudites leads to lower thermal conductivity as Sn is much lighter than the rare-earths (inset of Fig. 5). The explanation is the interaction of the low-frequency Sn-derived optical modes, *i.e.* the transverse Goldstone-like modes, with the heat-carrying acoustic phonons. As indicated in Fig. 3b, the acoustic phonons of $SnFe_4Sb_{12}$ are clearly truncated by (coupled with) the ultrasoft Sn-derived modes. This is seen in the three-phonon scattering phase space, which (as shown in Supplementary Fig. S1) is very large for $SnFe_4Sb_{12}$ at low frequencies when compared to $LaFe_4Sb_{12}$. The significantly increased three-phonon anharmonic scattering channels are responsible for reduction of phonon lifetime and thus ultralow κ_l. We note that thermal conductivity reduction due to proximity to a phase transition has been noted previously in the context of thermoelectrics.[41,42] The present result is distinct because as seen from the frequency of the longitudinal (highest frequency Sn related mode), and the energy scale for Sn off-centering (Fig. 2), $SnFe_4Sb_{12}$ is not particularly close to the phase transition.

Thus we find that $SnFe_4Sb_{12}$ has an ultralow thermal conductivity due to the interaction of very low frequency Sn-derived Goldstone-like modes with the acoustic modes of the host lattice. Unfortunately, from the point of view of thermoelectricity, $SnFe_4Sb_{12}$ is not a suitable composition. This is because Sn does not donate substantial charge to the $FeSb_3$ skutterudite framework and as a result the compound is too electron-deficient compared to the semiconducting composition $CoSb_3$. We verified this by electronic structure calculations (not shown).

As an aside, one may ask whether the physics discussed above could be useful in a feasible skutterudite composition for thermoelectrics. We emphasize that $SnFe_4Sb_{12}$ is unsuitable as a thermoelectric, in spite of its low thermal conductivity. This is a consequence of its electronic structure and electron count. In order to address this we explore the multiple filled skutterudite compositions with Sn and the highly electropositive La as fillers, $Sn_xLa_{1-x}Fe_4Sb_{12}$. This is motivated by the fact that La is known to donate electrons to $FeSb_3$, remedying its electron-deficient condition, $Sn_xLa_{1-x}Fe_4Sb_{12}$ or similar alloys may then show more suitable electronic properties, so it is of interest to see if Sn could lower the thermal conductivity in such cases. We perform supercell calculations for $Sn_xLa_{1-x}Fe_4Sb_{12}$ with different Sn-La ratios (x = 0.5 and 0.25) including structure relaxations and cal-
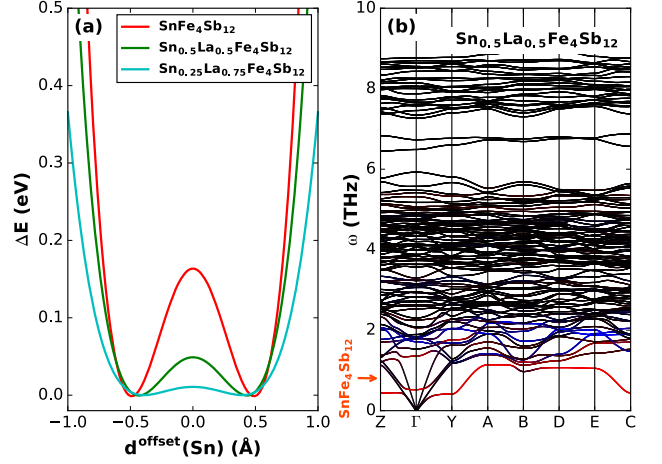

FIG. 6. (a) Calculated potential wells for Sn off-centering in double-filled skutterudites with Sn and La as fillers, $Sn_{0.5}La_{0.5}Fe_4Sb_{12}$ and $Sn_{0.25}La_{0.75}Fe_4Sb_{12}$. (b) Calculated phonon dispersion of $Sn_{0.5}La_{0.5}Fe_4Sb_{12}$. The blue and red lines indicate the projections onto the fillers of La and Sn, respectively. The orange arrow indicates the position of the lowest-frequency optical phonon at Γ in $SnFe_4Sb_{12}$.

culations of the potential energy well for Sn off-centering as described above for the pure Sn filled compound.

Results for the potential well are shown in Fig. 6 along with calculated phonons for the 50% Sn filled case $Sn_{0.5}La_{0.5}Fe_4Sb_{12}$. As seen, generally one observes similar double-well potentials for $Sn_xLa_{1-x}Fe_4Sb_{12}$, and the depth of the double-well potential decreases with the increasing amount of La substitution. The well becomes approximately flat for displacements up to 0.5 Å, for the 25% Sn filled case. Therefore the Sn off-centering picture still holds for such multiple filled skutterudites and Sn fillers are expected to contribute very low frequency vibrations over the whole composition range investigated. This is indicated in Fig. 6b, where $Sn_{0.5}La_{0.5}Fe_4Sb_{12}$ exhibits a Goldstone-like mode (red curve) with the even lower frequency (0.52 THz) than that of the pure Sn filled case (0.79 THz, indicated by orange arrow). In all cases, very low frequency modes and resulting strong reduction of the thermal conductivity is expected due to Sn addition.

VII. SUMMARY AND CONCLUSIONS

In summary, we find that Sn off-centers in the filled skutterudite $SnFe_4Sb_{12}$ due to rather strong interaction between Sn and the host lattice. However, in spite of this strong interaction, there are quite soft collective transverse modes that may be described as Goldstone-like modes associated with the Sn off-centering. These modes interact strongly with heat-carrying acoustic phonons leading to an ultralow lattice thermal conductivity. The results demonstrate a new way to reduce thermal conduc-

tivity in skutterudites and suggest experimental investigation of thermal properties of Sn-filled skutterudites, as well as measurements of the dynamics including Raman spectroscopy and phonon measurements by inelastic x-ray scattering or possibly neutron scattering if suitable samples become available. This provides a novel mechanism for thermal conductivity reduction by exploiting the complex physics of the lattice dynamics of solids, and illustrates a new feature of Goldstone physics in condensed matter.

* lijun_zhang@jlu.edu.cn
† singhdj@missouri.edu
[1] Y. Nambu, Phys. Rev. **117**, 648 (1960).
[2] J. Goldstone, Il Nuovo Cimento **19**, 154 (1961).
[3] C. A. Kendziora, I. A. Sergienko, R. Jin, J. He, V. Keppens, B. C. Sales, and D. Mandrus, Phys. Rev. Lett. **95**, 125503 (2005).
[4] B. C. Sales, D. Mandrus, and R. K. Williams, Science **272**, 1325 (1996).
[5] D. T. Morelli, G. P. Meisner, B. X. Chen, S. Q. Hu, and C. Uher, Phys. Rev. B **56**, 7376 (1997).
[6] G. P. Meisner, D. T. Morelli, S. Hu, J. Yang, and C. Uher, Phys. Rev. Lett. **80**, 3551 (1998).
[7] J. L. Feldman, D. J. Singh, I. I. Mazin, D. Mandrus, and B. C. Sales, Phys. Rev. B **61**, 9209 (2000).
[8] J. Yang, W. Zhang, S. Q. Bai, Z. Mei, and L. D. Chen, Appl. Phys. Lett. **90**, 192111 (2007).
[9] X. Shi, J. Yang, J. R. Salvador, M. F. Chi, J. Y. Cho, H. Wang, S. Q. Bai, J. H. Yang, W. Q. Zhang, and L. D. Chen, J. Am. Chem. Soc. **133**, 7837 (2011).
[10] J. Yang, L. Xi, W. Qiu, L. Wu, X. Shi, L. Chen, J. Yang, W. Zhang, C. Uher, and D. J. Singh, npj Computational Materials **2**, 15015 (2016).
[11] H. Luo, J. W. Krizan, L. Muechler, N. Haldolaarachchige, T. Klimzuk, W. Xie, M. K. Fuccilli, C. Felser, and R. J. Cava, Nature Comm. **6**, 6489 (2015).
[12] G. Xing, X. Fan, W. Zheng, Y. Ma, H. Shi, and D. J. Singh, Sci. Rep. **5**, 10782 (2015).
[13] M. Rasander, L. Bergqvist, and A. Delin, Phys. Rev. B **91**, 014303 (2015).
[14] Y. Fu, D. J. Singh, W. Li, and L. Zhang, Phys. Rev. B **94**, 075122 (2016).
[15] S. Lemal, N. Nguyen, J. de Boor, P. Ghosez, J. Varignon, B. Klobes, R. P. Hermann, and M. J. Verstraete, Phys. Rev. B **92**, 205204 (2015).
[16] W. Paschinger, G. Rogl, A. Grytsiv, H. Michor, P. R. Heinrich, H. Muller, S. Puchegger, B. Klobes, R. P. Hermann, M. Reinecker, C. Eisenmenger-Sitter, P. Broz, E. Bauer, G. Giester, M. Zehetbauer, and P. F. Rogl, Dalton Trans. **45**, 11071 (2016).
[17] G. Rogl, A. Grytsiv, P. Rogl, N. Peranio, E. Bauer, M. Zehetbauer, and O. Eibl, Acta Mater. **63**, 30 (2014).
[18] W. Schnelle, A. Leithe-Jasper, H. Rosner, R. Cardoso-Gil, R. Gumeniuk, D. Trots, J. A. Mydosh, and Y. Grin, Phys. Rev. B **77**, 094421 (2008).
[19] X. Tang, Q. Zhang, L. Chen, T. Goto, and T. Hirai, J. Appl. Phys. **97**, 093712 (2005).
[20] G. S. Nolas, D. T. Morelli, and T. M. Tritt, Annu. Rev. Mater. Sci. **29**, 89 (1999).
[21] X. Shi, W. Zhang, L. D. Chen, and J. Yang, Phys. Rev. Lett. **95**, 185503 (2005).
[22] B. Duan, J. Yang, J. R. Salvador, Y. He, B. Zhao, S. Wang, P. Wei, F. S. Ohuchi, W. Zhang, R. P. Hermann, O. Gourdon, S. X. Mao, Y. Cheng, C. Wang, J. Liu, P. Zhai, X. Tang, Q. Zhang, and J. Yang, Energy Env. Sci. **9**, 2090 (2016).
[23] H. Sellinschegg, S. L. Stuckmeyer, M. D. Hornbostel, and D. C. Johnson, Chem. Mater. **10**, 1096 (1998).
[24] G. S. Nolas, H. Takizawa, T. Endo, H. Sellinschegg, and D. C. Johnson, Appl. Phys. Lett. **77**, 52 (2000).
[25] P. Hohenberg and W. Kohn, Phys. Rev. **136**, B864 (1964).
[26] P. E. Blöchl, Phys. Rev. B **50**, 17953 (1994).
[27] G. Kresse and J. Furthmüller, Phys. Rev. B **54**, 11169 (1996).
[28] Z. G. Wu, R. E. Cohen, and D. J. Singh, Phys. Rev. B **70**, 104112 (2004).
[29] A. Togo and I. Tanaka, Scr. Mater. **108**, 1 (2015).
[30] W. Li, J. Carrete, N. A. Katcho, and N. Mingo, Comput. Phys. **185**, 1747 (2014).
[31] W. Li, L. Lindsay, D. A. Broido, D. A. Stewart, and N. Mingo, Phys. Rev. B **86**, 174307 (2012).
[32] W. Li and N. Mingo, Phys. Rev. B **89**, 184304 (2014).
[33] See Supplemental Materials at [link to be inserted by production] for details of calculations and associated information.
[34] G. S. Nolas, C. A. Kendziora, and H. Takizawa, J. Appl. Phys. **94**, 7440 (2003).
[35] M. Endres, T. Fukuhara, D. Pekker, M. Cheneau, P. Schauβ, C. Gross, E. Demler, S. Kuhr, and I. Bloch, Nature **487**, 454 (2012).
[36] D. Pekker and C. Varma, Annu. Rev. Condens. Matter Phys. **6**, 269 (2015).
[37] D. Podolsky, A. Auerbach, and D. P. Arovas, Phys. Rev. B **84**, 174522 (2011).

[38] L. Pollet and N. Prokof'ev, Phys. Rev. Lett. **109**, 010401 (2012).

[39] D. Podolsky and S. Sachdev, Phys. Rev. B **86**, 054508 (2012).

[40] W. Li and N. Mingo, Phys. Rev. B **91**, 144304 (2015).

[41] O. Delaire, J. Ma, K. Marty, A. F. May, M. A. McGuire, M. H. Du, D. J. Singh, A. Podlesnyak, G. Ehlers, M. D. Lumsden, and B. C. Sales, Nature Mater. **10**, 614 (2011).

[42] H. Liu, X. Yuan, P. Lu, X. Shi, F. Xu, Y. He, Y. Tang, S. Bai, W. Zhang, L. Chen, Y. Lin, L. Shi, H. Lin, X. Gao, X. Zhang, H. Chi, and C. Uher, Adv. Mater. **25**, 6607 (2013).